edge of the Gulf Stream and the secondary structure to the north. The three distinct gray shades that are visible indicate the presence of three definite thermal regions. The dark region to the east and south corresponds to the Gulf Stream; clouds (bright areas) obscure the warm waters of the stream farther seaward. The light gray area just east of the coast represents the cool (shelf) water mass, and the intermediate area represents the intermediate temperature of the slope water mass. Meanders in the Gulf Stream north wall (main boundary) are quite visible. These features have been observed from aircraft on previous occasions but only over very limited areas and never in a completely synoptic sense such as the satellite provides. Tongues of cool water penetrating into the intermediate slope water can also be noticed along the secondary thermal boundary. Pictures like this one can be received at any APT station and can be used operationally.

For quantitative work the digitized radiation information is more useful. When used for such studies the infrared radiation measurements should be corrected for any atmospheric contamination of the observed surface values. In the 10.5- to 12.5-μm region, atmospheric water vapor and carbon dioxide are absorbing constituents. Corrections vary with the viewing angle of observation, cloud conditions, and the amounts of these atmospheric constituents. The data presented in Fig. 1 have been corrected for these factors.

Figure 1 shows an analysis of the digitized infrared radiation data displayed on the cover. Isotherms have been drawn at intervals of 2°C. The 8°C isotherm traces, in gross fashion, the east coast of the United States, and a strong temperature gradient appears along the coastline. Over the Gulf Stream area the surface temperature was greater than 26°C, over the intermediate slope water about 20°C, and over the shelf waters about 17°C. The satellite-derived temperatures were compared with aircraft radiometric observations obtained over the same area on 17 October 1970 from the U.S. Naval Oceanographic Office. Differences were less than 1.0°C over the three principal water mass regions. The strong temperature gradient and the meanders along the main thermal boundary are very dramatic. Several interesting coastal water intrusions visible at various points on the cover are even more noticeable in Fig. 1. Two intrusions of cool shelf water penetrate the intermediate slope water just east of the James River and Chesapeake Bay. On each side of these cool tongues, a compensating intrusion of warmer water into the shelf waters toward the northwest is noticeable. Similar thermal features over the same area have been noticed on other days in the infrared radiation data from the satellite. A detailed analysis and interpretation of the satellite data and supporting surface information for these cases will be published at a later date.

Synoptic sea-surface temperature information from environmental satellites, together with supporting information from other observation platforms, can be very useful for increasing our understanding of the physical phenomena occurring over Earth's oceans. It is almost impossible to get an instantaneous and complete thermal picture of surface features with dimensions as large or larger than the Gulf Stream without use of environmental satellites equipped with infrared radiometers. Utilizing the satellite's capability to provide a synoptic overview of large portions of the ocean surface ties together the vertical soundings beneath the surface, possibly only from in situ measurements, for a more complete three-dimensional understanding of our marine environment.

P. K. Rao
A. E. Strong
R. Koffler

National Oceanic and Atmospheric Administration, National Environmental Satellite Service, Hillcrest Heights, Maryland 20031

References

1. P. C. Badgley, *Oceans from Space* (Gulf, Houston, 1969); W. R. Curtis and P. K. Rao, *J. Geophys. Res.* **74**, 6984 (1969); P. K. Rao, *Mar. Weather Log* **12**, 152 (1968); G. Warnecke, L. J. Allison, L. M. McMillin, K. Sekelda, *J. Phys. Oceanogr.* **1**, 45 (1971).
2. TOS Project/Goddard Space Flight Center, "ITOS" (Government Printing Office, Washington, D.C., 1970).

17 February 1971

Rifting in Iceland: New Geodetic Data

Abstract. *Small but measurable lengthening of several survey lines within the eastern rift zone of Iceland occurred between 1967 and 1970. The changes can be interpreted as a widening of the rift by 6 to 7 centimeters, possibly during the 1970 eruption of Hekla volcano.*

Fifty-eight survey lines averaging 2.7 km in length were measured with a model 6 Geodimeter in Iceland during 1967. Most of the lines were joined end to end to form two segmented profiles across the rift zones and were designed primarily to detect horizontal movements perpendicular to the rift axes (*1*). Resurvey of these lines was planned for 1972, but the May and June 1970 eruption of Mount Hekla, 15 km south of the eastern profile, prompted a resurvey of 17 line segments during September 1970 with a model 8 Geodimeter (Fig. 1).

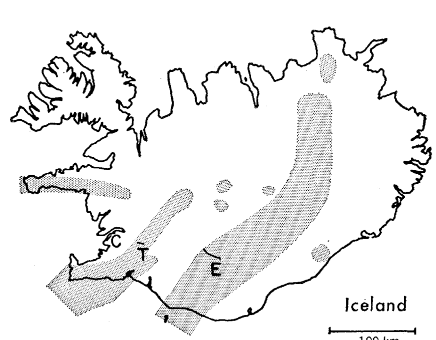

Fig. 1. Index map of Iceland showing the postglacial volcanic zones in gray (*12*) and three groups of survey lines: *C*, calibration lines; *T*, Thingvellir lines; *E*, eastern rift lines near Hekla volcano.

From Table 1 it can be seen that all the line segments show an apparent increase in length from 6 to 45 mm. These apparent increases are in part a problem of inaccuracy between the two different Geodimeters, which can fortunately be resolved. Two calibration lines were located in an aseismic area of Tertiary volcanics outside the rift zones and parallel to the northeast-southwest Tertiary dike trends. Therefore, for both geological and geophysical reasons, these lines can be considered relatively stable. An 18-mm correction is derived from the calibration data (Table 1); this correction can be subtracted from the 1970 values or added to the 1967 values. Statistical analysis of the 29 line differences exclusive of the calibration lines also indicates that there is a systematic rather than a random change with a mean difference of −20 mm and a standard error of the mean of 2 mm.

The differences between the 1967 values and the 1970 values, after the 18-mm calibration correction has been applied, are either random observational errors or are real changes in the lengths of the line segments. Figure 2 shows an analysis of the random error in duplicate measurements during 1967 and 1970 compared with the mean residual differences between the 1967 and 1970 data. The essential question is, how much of the change in line length is due to random error and how much, if any, is due to real displacement? Random measurement errors of 80 repeated observations made in 1967 and of 45 repeated observations made in 1970 have a normal distribution with a standard deviation of 5.7 mm. These values are similar to but largely independent of the random error shown in Fig. 2, A and B, and provide the estimate of variance used in the following statistical tests to evaluate the significance of the results: (i) The expected standard deviation of apparent changes from the sum of random errors in the 1967 and 1970 data is $5.7 \times \sqrt{2}$, or 8.1 mm. Thus, there is a probability of only .0048 that the +21-mm change between survey stations 3356 and 3357 is the sum of random measurement errors. (ii) A runs test for the number of changes in sign in the pattern of Fig. 2C yields a probability of .024 that the pattern is random. (iii) The systematic grouping of the five line segments between survey stations 3354 and 3359, which all show extension, is the strongest evidence for real change. The product of the probabilities that each of these values would occur or be exceeded on a random basis is less than 5×10^{-7}. Experience with the precision of survey lines measured by Geodimeters in California (*2*) and Hawaii (*3*) also indicates that a 5.7-mm standard deviation is reasonable for the random error in measuring lines 2 km in length. We conclude, therefore, that during the interval of 1967 to 1970 the survey profile in the eastern rift of Iceland shows small but measurable changes. Lines 3354 to 3359 show extension that ranges from 7 to 21 mm (± 8.1 mm) and lines 3350 to 3354 show contraction that ranges from 2 to 8 mm (± 8.1 mm). The extensions are significant, whereas the contractions are less than the precision of measurement. The systematic pattern of apparent changes (Fig. 2C and Fig. 3) also supports the conclusion that real displacements have been observed. In comparison, the four nearly identical survey lines across the north end of Lake Thingvellir (Table 1) show an average contraction of 2 mm (± 6 mm). The amount and random pattern of the changes at Lake Thingvellir during the interval 1967 to 1970 are clearly within the expected errors of measurement.

The north- and northeast-trending rift zones in Iceland have recently been interpreted in two distinctly different ways from geological evidence: (i) Gunnar Bödvarsson and Walker (*4*) and Nakamura (*5*) consider that the rifts are related to crustal extension perpendicular to the strike of the fractures, whereas (ii) Trausti Einarsson (*6*) considers that the en echelon pattern of rift fractures is related to shear motions that parallel the rift zones. The measured changes in line lengths northeast of Hekla can be interpreted by either hypothesis: (i) extension perpendicular to the rift could cause the measured changes, or (ii) left-lateral shear movements could result in shortening of lines 3350 to 3353 and of lines 3360 to 3361 and lengthening of lines 3353 to 3360.

Trausti Einarsson (*7*) interpreted the en echelon pattern of fractures near Hekla to be the result of right-lateral shear, opposite to the sense indicated by the measured changes. Because of this discrepancy and evidence favoring extensional rifting of the Mid-Atlantic Ridge immediately south of Iceland (*8*), we prefer the interpretation that

Table 1. Repeated measurements of slope distances between stations in 1967 and 1970.

Station	Station	Slope distances (m) 1967	Slope distances (m) 1970	Change (mm)
		Calibration lines		
D2	D1	5180.505	5180.518	13
		.500	.517	17
D2	D14	2956.566	2956.588	22
		.570	.590	20
		.560	.580	20
		Eastern rift lines		
3350	3351	2486.983	2486.994	11
		.983	.995	12
3352	3351	2288.880	2288.890	10
		.872	.894	22
3352	3353	2083.272	2083.289	17
		.278	.293	15
3354	3353	3047.491	3047.497	6
		.489	.502	13
3354	3355	3235.111	3235.136	25
		.112	.141	29
3356	3355	1850.952	1850.983	31
		.951	.981	30
3356	3357	1554.181	1554.214	33
		.169	.214	45
3358	3357	1292.746	1292.776	30
		.743	.763	20
3358	3359	2566.325	2566.357	32
		.323	.357	34
3360	3359	2497.360	2497.383	23
		.360	.376	16
3360	3361	1917.233	1917.248	15
		.233	.251	17
		Thingvellir lines		
5002	539	4895.315	4895.322	7
		.322	.333	11
5002	540	4965.048	4965.062	14
		.050	.068	18
5001	540	4950.483	4950.496	13
5001	539	4880.879	4880.903	24
		.880	.903	23

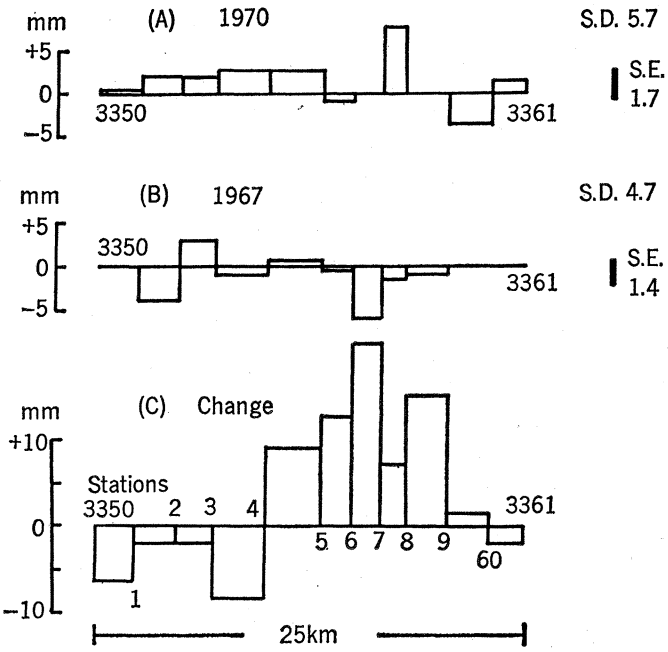

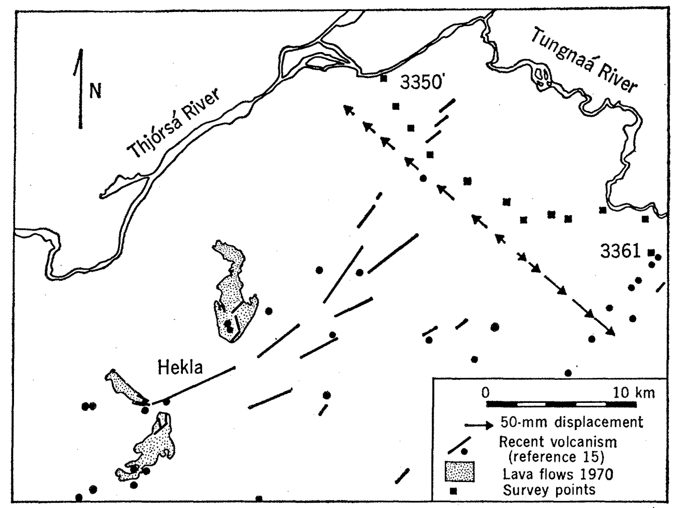

Fig. 2 (left). Measurement errors in 1970 and 1967 compared with the 1970 and 1967 changes in line lengths. On all graphs the horizontal scale is the distance between adjacent survey stations. (S.D., standard deviation; S.E., standard error of the mean.) (A) Precision of repeated measurements in 1970 on the 11 line segments from survey stations 3350 to 3361. Departure of the second measurement is shown in millimeters on the vertical scale compared with the average value of the two repeated measurements. (B) Precision of repeated measurements in 1967 as above. (C) The change between the mean distances measured in 1967 versus 1970 corrected for a calibration error of −18 mm on each 1970 distance. Fig. 3 (right). Location of the survey stations in the eastern rift zone of south central Iceland and the cumulative vectors of extension and contraction perpendicular to the rift zone needed to cause the measured changes in line length. A zero point is arbitrarily held between stations 3356 and 3357.

the changes in length are related to extension perpendicular to the rift zone (Fig. 3). The extension of the east rift zone indicated by the lengthening of lines 3354 to 3359 is 86 ± 24 mm. The indicated adjacent contraction of lines 3350 to 3354 is 20 ± 17 mm. The net apparent extension between stations 3350 to 3361 during the interval 1967 to 1970 is 65 ± 31 mm.

The 10-km-wide extension zone is 25 km northeast of Hekla volcano (Fig. 3), which erupted 200×10^6 m^3 of andesitic basalt during May and June 1970 (*9*). This extension zone is not in direct line with the trend of the Hekla fissure system, but about 10 km to the east of the trend. Preliminary analysis of earthquakes related in time to the Hekla eruption indicates some epicenters near the area where the measured extensions occurred. However, there is no direct evidence that the rifting is coincident with the Hekla eruption or the earthquakes.

The roles of various possible driving forces for plate tectonics remain uncertain. "Pull" from sinking lithosphere at converging plate margins, "drag" from currents along the plate bottoms or from internal body forces such as gravity sliding, or "push" from magmatic injection between separating plate margins are all possible mechanisms (*10*). At the European–North American plate boundary in Iceland, separation and rifting appear to result in both crustal extension and regional subsidence (*4, 11–13*). The occurrence of simultaneous extension and subsidence does not support a hypothesis that magmatic injection is causing the rifting. Increased pressure or volume of forcibly injecting magma would result in regional uplift and extension (*14*), although local collapse of a keystone-like block along the axis of the rift zone does occur on the active east rift of Kilauea volcano in Hawaii. More general collapse of rift zones can also result from removal of magma by surface eruption or subsurface migration, but this would occur after the initial phases of magmatic injection. More detailed knowledge of the sequence of ongoing horizontal and vertical movements of the ground surface over the Icelandic rift zones should provide some definite conclusions on the "push" versus "pull" or "drag" mechanisms.

In summary, we conclude that the small but significant extensions that occurred in the east rift zone of Iceland during the interval 1967 to 1970 support the hypothesis of plate tectonics and that future measurements of both horizontal and vertical ground-surface deformation on a more regional scale across active rift zones will provide important insight into the driving mechanisms of the separating plates.

R. W. DECKER
Dartmouth College,
Hanover, New Hampshire 03755
PÁLL EINARSSON
Lamont-Doherty Geological
Observatory, Columbia University,
Palisades, New York 10964
P. A. MOHR
Smithsonian Institution,
Astrophysical Observatory,
Cambridge, Massachusetts 02138

References and Notes

1. R. W. Decker, *Trans. Am. Geophys. Union* **49**, 114 (1968); *Am. Phil. Soc. Yearb.* **1967**, 258 (1967).
2. R. B. Hofmann, *Calif. Dep. Water Resour. Bull. 116-6* (1968).
3. W. T. Kinoshita, personal communication.
4. Gunnar Bödvarsson and G. P. L. Walker, *Geophys. J. R. Astron. Soc.* **8**, 285 (1964).
5. K. Nakamura, *Nat. Isl.* **2**, 8, 1 (1970).
6. Trausti Einarsson, *J. Geophys. Res.* **73**, 7561 (1968).
7. ———, *Soc. Sci. Isl.* **38**, 128 (1967).
8. M. Talwani, C. C. Windisch, M. G. Langseth, Jr., *J. Geophys. Res.* **76**, 473 (1971); L. R. Sykes, *ibid.* **72**, 2131 (1967).
9. Sigurdur Thorarinsson, *Hekla, a Notorious Volcano* (Almenno, Reykjavik, 1970).
10. G. P. L. Walker, *Phil. Trans. R. Soc. London Ser. A* **258**, 199 (1965); D. P. McKenzie, *Geophys. J.* **18**, 1 (1969); L. Lliboutry, *J. Geophys. Res.* **74**, 6525 (1969).
11. W. R. Jacoby, *J. Geophys. Res.* **75**, 5671 (1970).
12. Eysteinn Tryggvason, *ibid.* **73**, 7039 (1968).
13. ———, *ibid.* **75**, 4407 (1970).

14. K. Mogi, *Bull. Earthquake Res. Inst. Tokyo Univ.* **36**, 99 (1958); J. B. Walsh and R. W. Decker, *J. Geophys. Res.* **76**, 3291 (1971).
15. Gudmundur Kjartansson, *Geological Map of Iceland* (Museum of Natural History, Reykjavik, 1962), sheet 6.
16. We thank J. Peirce, W. Walker, and J. Decker for their assistance with the fieldwork, Gudmundur Sigvaldason and Gudmundur Pálmason for their continuing help and advice, and V. McGee for his aid with the statistical tests. Supported by the American Philosophical Society and NSF grants GA-965 (1967) and GA-2686 (1970).

11 March 1971; revised 6 May 1971

Quartz: Synthesis at Earth-Surface Conditions

Abstract. *Quartz has been crystallized directly from seawater at room temperature. This is the first time that identifiable quartz has been synthesized in aqueous solution at earth-surface conditions without the aging of an original amorphous precipitate. The concentration of dissolved silica in equilibrium with quartz at 20°C and 1 atmosphere is 4.4 ± 0.3 parts per million, a value in agreement with the theoretical value obtained by a constant heat capacity fit of higher temperature equilibrium data. This experiment confirms the results of petrologic investigations which suggest that quartz precipitates directly from aqueous solution during chemical weathering and early diagenesis.*

Quartz has been considered to be chemically "inert" in most environments at or near the earth's surface. It has been assumed that, at temperatures below 100°C, the formation of quartz from supersaturated solutions or from amorphous silica requires thousands of years. The dissolution of quartz in unsaturated solutions at most earth-surface conditions is slow (*1*, *2*). However, quartz-cemented sandstones, secondary quartz rimming of Recent lacustrine quartz sands, and quartz crystals found in weathering profiles are interpretable as precipitates of quartz from aqueous solution at earth-surface conditions formed in a relatively short time (*3*).

Recently, quartz has been synthesized over the temperature range from 0° to 80°C by the aging of amorphous hydroxide-silica precipitates of iron (Fe^{3+}) and other elements in the presence of aqueous solutions (*2*). Morey *et al.* (*4*) obtained supersaturated solutions of silica by the continuous agitation of a suspension of quartz grains in water. In one experiment the solution reached a concentration of 80 parts per million (ppm) of dissolved silica after 386 days of agitation, and subsequently the concentration dropped

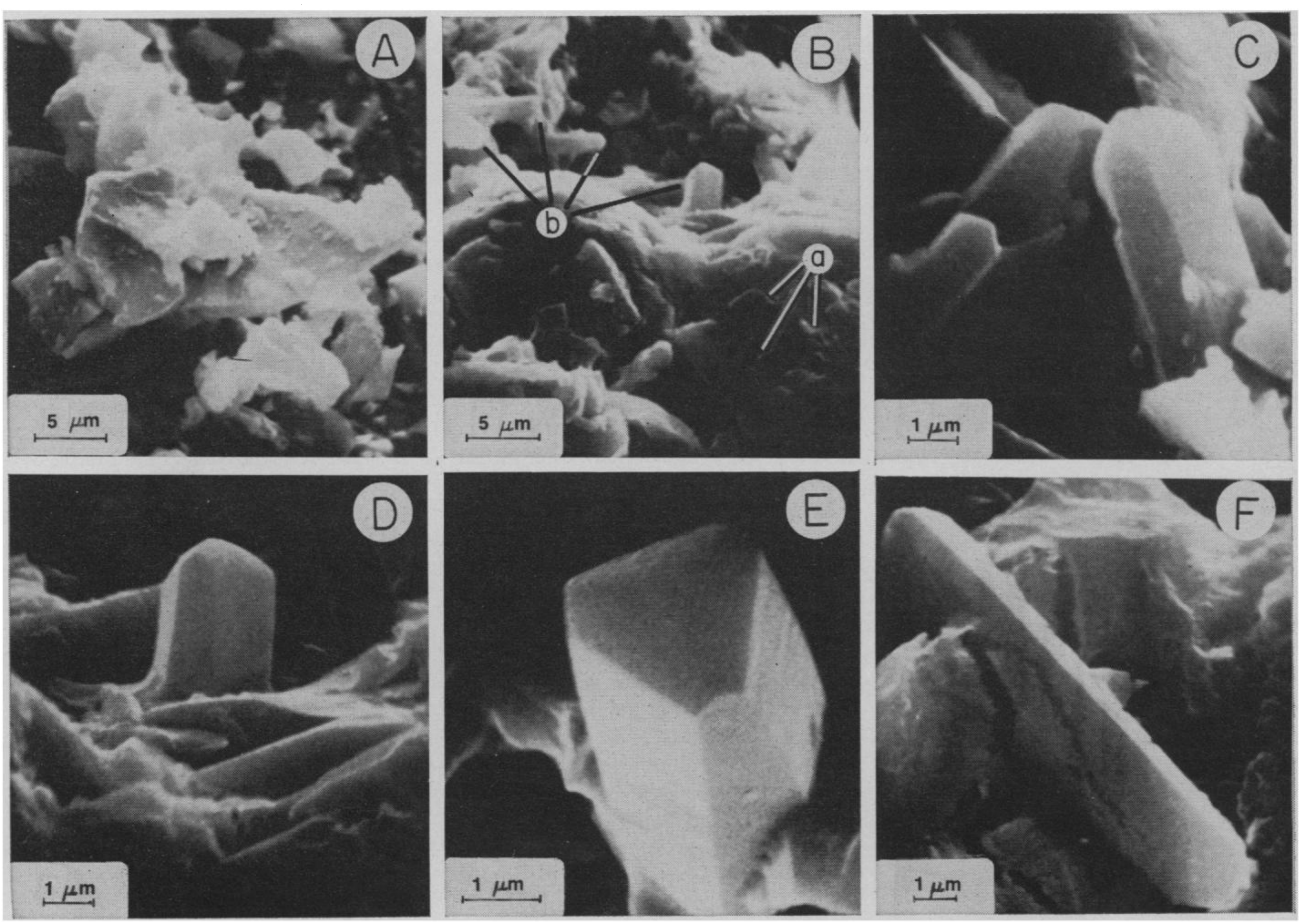

Fig. 1. Scanning electron photomicrographs. (A) Ground quartz material obtained by grinding a single crystal of quartz. Note the high angularity and poor sorting of the particles. (B) On the surface of the ground quartz material after reaction, V-shaped solution pits (*a*) have developed. Several authigenic quartz crystals (*b*) are seen in the upper portion of the photograph. (C) Authigenic quartz crystals converging toward the center of the photomicrograph. (D) Crystal of authigenic quartz developed on a conchoidal breakage pattern of the ground material. (E) Authigenic quartz displaying striations parallel to (0001) on the prism faces and the tapering of a $10\bar{1}0$ prismatic face. (F) Authigenic quartz crystal with double terminations, about 10 µm in length.